

Angular dependence of microwave dissipation by vortices in $\text{YBa}_2\text{Cu}_3\text{O}_{7-x}$ thin films

N. Anand and M. Tinkham

Department of Physics and Division of Applied Sciences, Harvard University, Cambridge, Massachusetts 02138

(Received 1 March 1995)

Using meander line resonant structures, we perform highly sensitive measurements of the changes in surface resistance ΔR_s of $\text{YBa}_2\text{Cu}_3\text{O}_{7-x}$ thin films in order to probe the vortex dynamics as a function of temperature, applied dc magnetic field, and angle (θ) of the applied field relative to the ab planes. We observe that the component of the magnetic field normal to the planes produces substantially more dissipation than the component parallel to the planes. By using an extension of the London theory to anisotropic superconductors, we can calculate the internal flux densities parallel (B_{ab}) and perpendicular (B_c) to the ab planes inside a superconductor for an arbitrary field orientation relative to the ab planes. For low fields, we can define a weight (δ) of the contribution to dissipation from B_{ab} relative to that from B_c . This allows us to calculate an "effective" internal flux density and hence obtain the total dissipation. Using the results from this theory, we obtain excellent quantitative agreement with our measurements of ΔR_s vs θ .

I. INTRODUCTION

Surface impedance (Z_s) measurements at microwave frequencies are playing an important role in exploring the properties of the superconducting mixed state in high-temperature superconductors.¹⁻³ The imaginary part of the surface impedance, the surface reactance, is directly related to the magnetic penetration depth λ , which provides a measure of the superfluid density, the temperature dependence of which reflects the quasiparticle density of states available for thermal excitations and therefore probes the gap structure of the superconducting state.⁴ The real part of the surface impedance, the surface resistance, describes microwave power losses and can yield useful information about vortex dynamics in these materials.

A proper understanding of the material characteristics at high frequencies is also necessary for some applications of high-temperature superconductors which require low surface impedance in the presence of strong dc and rf magnetic fields. As a result, there has been much interest in the vortex state properties of high-temperature superconductors. In particular it is important to have a good understanding of the mechanisms for the field dependence of Z_s .

Radio-frequency surface resistance (R_s) measurements have most often been performed using resonant cavities. Typically these measurements involve either replacing one end face of a cylindrical cavity (usually made of copper or niobium) by the film under test,⁵ or placing the film inside the cavity at a location where the rf magnetic field is a maximum.⁶ Another way of making R_s measurements is to use planar transmission line resonators. Using these structures, one can easily measure changes in R_s as a function of frequency, temperature, rf, and dc magnetic fields.^{7,8}

In the research reported in this paper, we use a planar transmission line structure (microstripline resonator) to

study the role of anisotropy in microwave dissipation due to vortices in c -axis oriented $\text{YBa}_2\text{Cu}_3\text{O}_{7-x}$ (YBCO) thin films as a function of temperature and field orientation relative to the ab planes. In order to have a quantitative understanding of the data on angular dependence of dissipation on field, it is essential to know the magnitude of the internal flux densities both parallel and perpendicular to the ab planes. Some of the theoretical background along with the main results essential for our analysis are outlined in the theory section that follows.

II. THEORY

The anisotropic effective mass formulations of the Ginzburg-Landau (GL) and London theories⁹ can be used to calculate the effective thermodynamic parameters such as H_{c1} , H_{c2} , and the vortex line energy as angular dependent quantities. Further, for three-dimensional anisotropic superconductors for field applied in any direction except along the principal axes, both theories predict the existence of a transverse magnetization (perpendicular to B) in addition to the usual longitudinal magnetization (along B) in the mixed state. The physical origin of the transverse magnetization in an anisotropic superconductor can be seen in the following argument: a consequence of the anisotropic mass tensor is that the currents will have both "easy" and "hard" directions of flow. The easy direction is that in which the effective mass is a minimum. Consequently, the kinetic part of the GL free energy for a given current density is a minimum for this direction. Hence, because of energy considerations, the currents associated with a vortex will not in general flow in a plane orthogonal to the vortex direction. In the case of the high- T_c systems, the currents will flow preferentially in the CuO planes. For the internal field (B) oriented at an angle θ relative to the ab planes, the currents will produce a magnetic moment which is at an

angle θ_M from the ab plane such that

$$\tan \theta_M = \gamma^2 \tan \theta, \quad (1)$$

where γ^2 is the anisotropic mass ratio [$\gamma^2 = m_c/m_{ab}$, where m_c (m_{ab}) is the effective mass along the c axis (ab plane)]. Therefore, if a field is applied at some angle other than 0° or 90° , the currents will flow in a plane which is close to the ab plane and the magnetic moments associated with these canted current loops will produce transverse magnetization. In the broad field range where $H_{c1} \ll H \ll H_{c2}$, one can assume both a nearly constant order parameter (the large value of κ implies that the cores are small and widely spaced) and nearly uniform field penetration (the vortices overlap). These assumptions allow the use of the London approximation and also assure that $B \approx H \gg |M| \sim H_{c1}$. As shown by Kogan and his collaborators,⁹ this inequality allows the analysis to be simplified by neglecting the demagnetizing fields (which are of order M), and also to a good approximation allows neglecting all terms higher than linear in M . By using the London equations with an anisotropic mass tensor, they obtain

$$B_c = H \sin \theta \left(1 - \frac{H^*}{H} \frac{\gamma^2}{\sqrt{\cos^2 \theta + \gamma^2 \sin^2 \theta}} \right), \quad (2)$$

$$B_{ab} = H \cos \theta \left(1 - \frac{H^*}{H} \frac{1}{\sqrt{\cos^2 \theta + \gamma^2 \sin^2 \theta}} \right), \quad (3)$$

where

$$H^* = \frac{\Phi_0}{8\pi\lambda_{ab}^2} \ln \left(\frac{\beta H_{c2}(T, \theta)}{B} \right). \quad (4)$$

Here B_c (B_{ab}) refer to the component of B perpendicular (parallel) to the ab planes and θ is the angle between the direction of B , and the ab planes. The in-plane penetration depth is λ_{ab} , Φ_0 is the superconducting flux quantum (2×10^{-7} G cm²), β is a factor (~ 1) which results from an integral cutoff in the theory, and $H_{c2}(T, \theta)$ is the temperature- and angle-dependent upper critical field. It should be noted that in an experiment, the angle that is controlled is not exactly θ but rather θ_a (the angle between the applied field direction and the ab plane). The difference between θ and θ_a is of order M/H , which for fields large compared to H_{c1} is small, and it will be ignored in the treatment of the experimental data discussed in this paper.

III. EXPERIMENT

A. Resonator characteristics

To measure changes in R_s for YBCO thin films we use the microstripline resonator structure shown in Fig. 1. A microstripline has a patterned strip film and a ground plane, with a dielectric separating the two conductors. We use a normal-metal ground plane (copper) with a LaAlO₃ substrate as a dielectric ($\epsilon \approx 25$) separating the

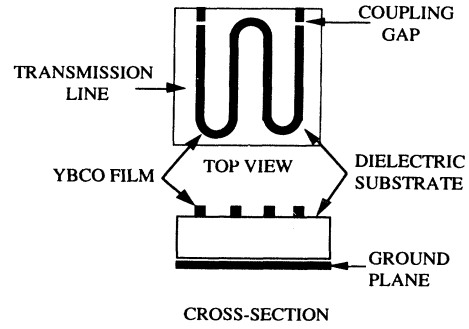


FIG. 1. Schematic view of the microstripline resonator showing a simplified view of the meander line structure, with top view and cross section showing the transmission line and the coupling gaps of the resonator structure.

ground plane and the YBCO film¹⁰ (thickness ≈ 3500 Å). The frequency for which the line is one-half wavelength long is the fundamental frequency of the resonator and overtone resonances occur at integral multiples of the fundamental frequency. The chosen length of the line yields a fundamental frequency of approximately 0.8 GHz. We pattern a YBCO film using standard photolithographic techniques and wet etching in a dilute solution of phosphoric acid. The linewidth of the patterned film is about $150 \mu\text{m}$ and the dimensions of the dielectric substrate are $1 \times 1 \times 0.05$ cm³. These dimensions yield a transmission line with a characteristic impedance¹¹ of approximately 50Ω . Our resonator is capacitively coupled to the external circuit across gaps at the two ends of the patterned YBCO film.

The measured quality factor Q (i.e., the loaded Q) of the resonator is given by

$$\frac{1}{Q} = \frac{1}{Q_{\text{ex}}} + \frac{1}{Q_d} + \frac{1}{Q_{\text{gnd}}} + \frac{1}{Q_{\text{sc}}}. \quad (5)$$

Q_{ex} represents the external loading of the resonator and can be adjusted by varying the coupling to the external circuit. Q_d and Q_{gnd} represent the losses in the dielectric and the copper ground plane. Q_{sc} represents the losses in the superconducting YBCO film and is inversely proportional to the rf surface resistance of the film ($1/Q_{\text{sc}} \propto R_s$). Since we are interested in measuring Q_{sc} , we want to minimize the losses from all other sources compared to the losses in the YBCO film. By using a low loss dielectric and by being in the weak-coupling limit, we have $Q_d \gg Q_{\text{sc}}$ and $Q_{\text{ex}} \gg Q_{\text{sc}}$, which leads to $Q^{-1} \approx Q_{\text{sc}}^{-1} + Q_{\text{gnd}}^{-1}$. Thus the measured Q is primarily limited by losses in the conductors and not by external factors such as losses in the dielectric or external coupling. This gives us a high value of Q and consequently high sensitivity. By measuring the changes in $1/Q$ relative to the zero applied field case for a given temperature, we can subtract out the loss contribution from the copper ground plane. In this fashion, we can relate the measured $1/Q$ values directly to the change in surface resistance of the YBCO film due to an applied field.

B. Experimental setup

Microwave dissipation measurements are performed as a function of temperature, field strength, and field orientation. The patterned film is mounted on a copper stage which also serves as the ground plane. This package is mounted in a cryostat, where the sample temperature can be varied from 77 to 300 K. The temperature is measured with a platinum resistor which is attached to the copper stage, and it is stabilized to within ± 0.005 K using a Lakeshore DRC-91A temperature controller. A dc magnetic field is applied using a Varian V-3603 low impedance electromagnet. The magnet has a lockable base ring which permits 360° rotation of the magnet, allowing us to vary the field angle with respect to the ab planes. The angular accuracy using this setup is $\sim 0.5^\circ$. Our measurement routine is the following. For a given field orientation and field strength, the thin film is cooled from above T_c down to 78 K. The temperature is increased in steps of 0.1 K and after each increase, we wait for a few minutes to allow the temperature to equilibrate before making the next Q measurement.

Microwave energy is coupled to the system through two coaxial leads. We performed all the microwave measurements discussed in this paper at 0.8 GHz (the fundamental transmission resonance of the resonator) using a Hewlett Packard 8510B vector network analyzer. For each temperature of interest, we use a computer to program the network analyzer to sweep over a frequency range spanning the fundamental transmission resonance of the resonator. From these data, we determine the resonant frequency ω_0 and the peak height (there is almost no transmitted power far off resonance, so we take the background transmission to be zero). The computer then determines the separation $\Delta\omega$ of the frequencies corresponding to the half maximum points of the transmission resonance, and computes the Q ($= \omega_0/\Delta\omega$) of the transmission resonance. As the temperature is increased, the resonant frequency shifts to lower frequencies (because the penetration depth increases as a function of temperature). We track this shift of frequency, and adjust our frequency window to track the peak such that the transmission resonance is always centered in our frequency window. This entire procedure, i.e., data acquisition from the network analyzer and the temperature controller and the tracking of the resonance peak, is fully computer controlled. Each temperature sweep typically takes about 6 h to complete. Then the field orientation is changed by manually rotating the electromagnet and the above procedure is repeated for the new field orientation. From this set of data, we can extract the angular dependence of the change in field-cooled surface resistance (ΔR_s) for any given temperature.

IV. RESULTS

A. Dissipation due to field parallel and perpendicular to the ab planes

Figure 2 shows $1/Q$ ($\propto R_s$) as a function of temperature for a YBCO film for a field of 500 G applied perpen-

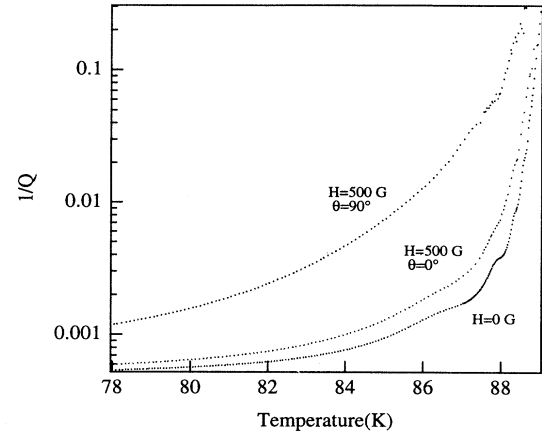


FIG. 2. $1/Q$ versus temperature (at approximately 0.8 GHz) showing that fields perpendicular to the ab planes give the dominant contribution to the dissipation. The topmost curve is for a dc magnetic field (500 G) applied perpendicular to the planes. The middle curve is for the same field applied parallel to the ab planes. For reference, we also show the data for zero applied field (bottom curve).

dicular (top curve) and parallel (middle curve) to the ab planes. For reference, the zero-field data is also shown (bottom curve). We note that the orientation of the field relative to the ab planes causes a substantial difference in the dissipation.¹² The field-induced increase in dissipation relative to the zero field value is about 15 times higher for the field normal to the planes than for the field parallel to the planes. In order to gain insight into where this factor of 15 comes from, it is useful to consider the forces exerted on the flux lines by the rf currents flowing in the resonator. For fields parallel to the planes, the rf currents (flowing in the planes perpendicular to the field, see Fig. 3) exert a driving force parallel to the c axis, i.e., they try to push the flux lines across the planes. However, for fields perpendicular to the ab planes, the driving force on the flux lines lies in the ab plane. Because of the anisotropy of the upper critical field ($H_{c2\parallel}/H_{c2\perp} = \gamma \approx 7$), we have an anisotropic Bardeen-Stephen coefficient of viscous drag ($\eta_{\parallel}/\eta_{\perp} = \gamma$).

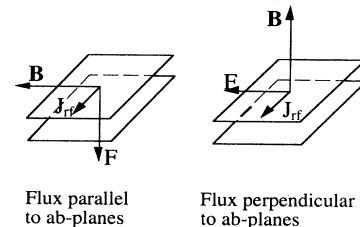


FIG. 3. Forces acting on a flux line for the parallel and perpendicular case. B , J_{rf} , and F represent the magnetic field, rf current, and the driving force on the flux line due to the rf current.

Thus we would expect higher dissipation for fields oriented perpendicular to the planes compared to fields parallel to the planes. The anisotropy of H_{c2} partially accounts (factor of $\gamma \sim 7$) for the difference (factor ~ 15) in dissipation. This suggests that some other effect may also contribute to the anisotropy of dissipation, e.g., intrinsic pinning due to the layered structure of the material.¹³

B. Angular dependence of dissipation

For a given value of the applied field (H) and its angle (θ) relative to the ab planes, using Eqs. (2) and (3) we can calculate the internal flux densities (B) parallel and perpendicular to the planes as a function of the parameter β and other parameters which are known *a priori*. As discussed above, these two components of \mathbf{B} do not contribute equally to the dissipation. We can define a relative weight δ of the contribution from B_{ab} relative to that from B_c as

$$\delta(T) = \frac{R_s(T, H_{\parallel}) - R_s(T, H = 0)}{R_s(T, H_{\perp}) - R_s(T, H = 0)}, \quad (6)$$

i.e., for a given temperature T and field H , δ is the ratio of the change in dissipation (relative to the zero field case, see Fig. 2) for field parallel (H_{\parallel}) and perpendicular (H_{\perp}) to the planes.

This definition can be used at low fields, i.e., for the applied field H less than some “threshold” field H_{th} . This definition for δ relies on having H aligned parallel and perpendicular to the planes. For fields applied parallel to the planes, due to the finite accuracy in field alignment, the field direction is probably not strictly parallel to them, but is in fact inclined at some small angle. However, if the applied field is small enough (i.e., $H < H_{th}$), it can be completely shielded from the ab planes and is forced to lie parallel to them (transverse Meissner effect¹⁴). Equation (6) cannot be used for $H > H_{th}$ because in this field regime the nominally “parallel” field case also has field crossing the ab planes because of imprecise alignment, thus making it impossible to measure the dissipation arising from just the parallel component. For fields applied at an angle of 0.5° from the ab planes of our samples at 78 K, H_{th} is found to be about 1 kG.¹⁴ For the measurements reported in this paper, the fields used (500 and 100 G) are well below H_{th} .

Using δ , we can calculate an “effective” flux density in order to determine the total dissipation produced by a field at an arbitrary angle from the ab planes. We find that we can model the measured change in dissipation relative to the zero field case as follows:

$$\begin{aligned} \Delta R_s(H, \theta) &= R_s(H, \theta) - R_s(H = 0) \\ &= A \sqrt{B_c^2(H, \theta) + \delta^2 B_{ab}^2(H, \theta)}, \end{aligned} \quad (7)$$

where A is a proportionality constant (this reduces properly to the isotropic superconductor in the limit δ approaches 1). We can define A as follows:

$$A = \frac{R_s(H, \theta = 90^\circ) - R_s(H = 0)}{B_c(H, \theta = 90^\circ)}, \quad (8)$$

i.e., we are normalizing to the perpendicular field data where $B_{ab}(H, \theta = 90^\circ)$ is zero.

Figure 4 shows the angular dependence of the change in surface resistance (relative to the zero-field surface resistance for that temperature) as a function of the angle of the applied field relative to the ab planes for several fixed temperatures. Using Eq. (8) along with the expressions for B_{ab} and B_c from Eqs. (2) and (3) in Eq. (7), we have an expression for ΔR_s in terms of the parameter $\beta H_{c2}(\theta, T)$. We can explicitly take account of the known¹⁵ temperature and angular dependence of H_{c2} [$H_{c2} \equiv H_0 F(\theta, T)$] and substitute this in Eq. (7) to obtain an expression for ΔR_s in terms of βH_0 , a temperature- and angle-independent quantity. Now we can fit the data at one temperature using βH_0 as the *single* fitting parameter (the fit for $T = 81$ K is shown in Fig. 4 as a solid curve). This fixes a value of βH_0 which we can then use to generate the predicted dependence for all other temperatures and angles without any free parameters. The predictions are shown in Fig. 4 as dashed curves, which are in excellent agreement with our data for all the temperatures. Similar measurements were also performed for a smaller field ($H = 100$ G). We observed similar agreement of the fits with the data.

As a test of uniqueness of this theoretical model, we have tried to fit the data shown in Fig. 4 using other “plausible” fitting functions. For instance, if we assume that the entire contribution to the dissipation comes from

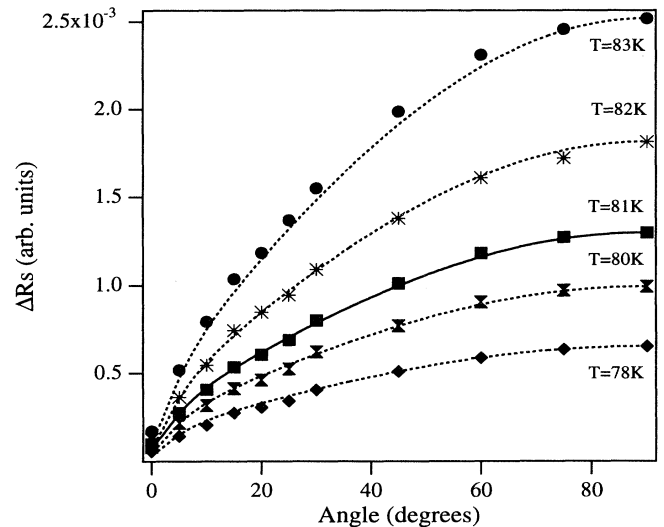


FIG. 4. Change in surface resistance (measured relative to the zero-field value for each temperature) versus angle (at 0.8 GHz) for an applied field of 500 G for various temperatures. Using the results from anisotropic London theory with an appropriate weighting factor [δ , see Eq. (6)], we fit the data for $T=81$ K (solid curve) using one free parameter. The dashed curves are predictions (without *any* free parameters) for the other temperatures based on the value from the 81 K fit.

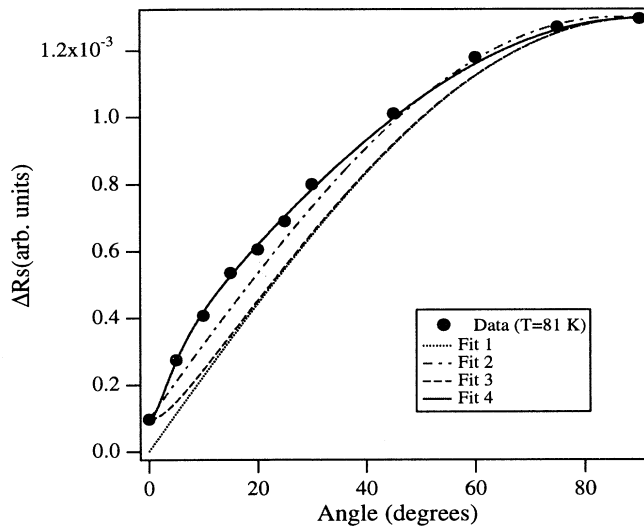


FIG. 5. Change in surface resistance (ΔR_s) relative to the zero field case for $T = 81$ K vs angle for an applied field of 500 G. Also shown are fits to the data using various fitting functions. Fit 1 uses a sinusoidal dependence of ΔR_s on θ . Fits 2 and 3 use $\Delta R_s \propto (\sin \theta + \delta \cos \theta)$ and $\Delta R_s \propto (\sin^2 \theta + \delta^2 \cos^2 \theta)^{1/2}$. Fit 4, the same as in Fig. 4, uses the model developed in the text.

the component of the field perpendicular to the ab planes, and that this component is proportional to $\sin \theta$ (i.e., neglecting screening of the field), then our data should show a simple sinusoidal dependence on the angle of the applied field. This function is compared with the 81 K data in Fig. 5. We have also tried linear and quadratic combinations of sine and cosine of the angle of the applied field along with the weighting factor δ [see Eq. (6)] multiplying the cosine term (i.e., now both components of the field contribute, but we are still ignoring the screening of

the field). As is clear from Fig. 5, none of these three alternative approaches yield good agreement with the data.¹⁶ Good agreement of the fits with the data cannot be obtained¹⁷ without taking account of the anisotropy in the angular dependence of the *internal* flux density [Eqs. (2) and (3)] and by giving appropriately reduced weight [Eq. (6)] to the parallel component of the flux density relative to the perpendicular component.

V. CONCLUSION

Using a microstripline resonator structure, we have made sensitive measurements of changes in surface resistance as a function of temperature and of the strength and angle of the magnetic field with respect to the ab plane for YBCO thin films. By using an extension of the London theory to anisotropic superconductors, we can calculate the internal fields of a superconductor for an arbitrary field orientation relative to the ab planes. Using the results from this theory, we obtain excellent quantitative agreement with our data. For low fields, using the weight factor (δ) of the contribution from B_{ab} relative to that from B_c , we can calculate the “effective” internal flux density and obtain the total dissipation. We observe excellent agreement of our predictions with the data, but not with other plausible approximations which do not take account of the anisotropic screening of the internal flux density.

ACKNOWLEDGMENTS

The authors wish to thank M. A. Itzler and R. J. Fitzgerald for helpful discussions. This research was supported in part by MRSEC Grant No. DMR-94-00396 and by NSF Grant No. DMR-92-07956.

¹ N.-C. Yeh, U. Kriplani, W. Jhiang, D. S. Reed, D. M. Strayer, J. B. Barner, B. D. Hunt, M. C. Moore, R. P. Vasquez, A. Gupta, and A. Kussmaul, *Phys. Rev. B* **48**, 9861 (1993).
² J. Owliaei, S. Sridhar, and J. Talvacchio, *Phys. Rev. Lett.* **69**, 3366 (1992).
³ Balam A. Willemsen, S. Sridhar, John S. Derov, and Jose Silva, *Appl. Phys. Lett.* (to be published).
⁴ W. N. Hardy, D. A. Bonn, D. C. Morgan, Ruixing Liang, and Kuan Zhang, *Phys. Rev. Lett.* **73**, 2484 (1993).
⁵ N. Klein, G. Muller, H. Piel, B. Roas, L. Schultz, U. Klein, and M. Peiniger, *Appl. Phys. Lett.* **54**, 757 (1989).
⁶ D. L. Rubin, K. Green, J. Gruschus, J. Kirchgessner, D. Moffat, H. Padamsee, J. Sears, Q. S. Shu, L. F. Schneemeyer, and J. V. Waszczak, *Phys. Rev. B* **38**, 6538 (1988).
⁷ Steven M. Anlage, Hsuan Sze, Howard J. Snortland, Shuichi Tahara, Brian Langley, Chang-Beom Eom, M. R. Beasley, and Robert Taber, *Appl. Phys. Lett.* **54**, 2710 (1989).

⁸ D. E. Oates, A. C. Anderson, and P. M. Mankiewich, *J. Supercond.* **3**, 251 (1990).
⁹ V. G. Kogan, *Phys. Rev. B* **24**, 1572 (1981); V. G. Kogan and J. R. Clem, *ibid.* **24**, 2497 (1981); L. J. Campbell, M. M. Doria, and V. G. Kogan, *ibid.* **38**, 2439 (1988); V. G. Kogan, *ibid.* **38**, 7049 (1988).
¹⁰ Obtained from Conductus, Sunnyvale, CA.
¹¹ See, for example, P. A. Rizzi, *Microwave Engineering Passive Circuits* (Prentice-Hall, New Jersey, 1988).
¹² M. Golosovsky, M. Tsindlekht, H. Chayet, and D. Davidov, *Phys. Rev. B* **50**, 470, (1994); M. Golosovsky, D. Davidov, E. Farber, T. Tsach, and M. Schieber, *ibid.* **43**, 10390 (1993).
¹³ W. K. Kwok, U. Welp, V. M. Vinokur, S. Flesher, J. Downey, and G. W. Crabtree, *Phys. Rev. Lett.* **67**, 390 (1991).
¹⁴ N. Anand, M. A. Itzler, and M. Tinkham, *IEEE Trans. Supercond.* (to be published).
¹⁵ We use the following dependence of H_{c2} on t ($= T/T_c$) and θ : $H_{c2\parallel ab} \propto (1-t)$ and $H_{c2}(\theta) = H_{c2\parallel ab}(\cos^2 \theta +$

$$\gamma^2 \sin^2 \theta)^{-1/2}.$$

¹⁶ For the fits shown in Fig. 5, δ as defined in Eq. (6) is used. For fits 2 and 3 this definition of δ automatically forces the fits to pass through the 0° data point. However, for fit 4, for the fit to agree with the data at 90° and 0° , we would need to use $\delta'(T) = \delta(T)[B_c(90^\circ)/B_{ab}(0^\circ)]$. We prefer to use the definition of δ as defined in Eq. (6) as it is more

intuitive and it causes only a small deviation from the value at 0° .

¹⁷ We get comparable agreement of the fit with our data if we assume that the net dissipation is simply a sum of the dissipation arising from the two components, i.e., $\Delta R_s(H, \theta) = A[|B_c(H, \theta)| + \delta|B_{ab}(H, \theta)|]$.